NANO LETTERS

LETTER

pubs.acs.org/NanoLett

Plasmonic Nanobilliards: Controlling Nanoparticle Movement Using Forces Induced by Swift Electrons

P. E. Batson,[*,†] A. Reyes-Coronado,[‡,§,∥] R. G. Barrera,[⊥] A. Rivacoba,[‡,#,¶] P. M. Echenique,[‡,#,¶] and J. Aizpurua[‡,¶]

[†]Institute for Advanced Materials, Devices, and Nanotechnology, Rutgers University, Piscataway, New Jersey 08854, United States

[‡]Donostia International Physics Center, "DIPC", Donostia-San Sebastian, 20018, Spain

[§]Centro de Ciencias Aplicadas y Desarrollo Tecnológico, Universidad Nacional Autónoma de México, 01000, México D.F., Mexico

[∥]Institute of Electronic Structure and Laser (IESL), Foundation for Research and Technology Hellas (FORTH), P.O. Box 1385, 71110 Heraklion, Crete, Greece

[⊥]Instituto de Física, Universidad Nacional Autónoma de México, 01000 México D.F., Mexico

[#]Universidad del País Vasco (UPV)/EHU, Donostia-San Sebastian, 20018, Spain

[¶]Centro de Física de Materiales CSIC-UPV/EHU, Donostia-San Sebastian, 20018, Spain

Supporting Information

ABSTRACT: Manipulation of nanoscale objects to build useful structures requires a detailed understanding and control of forces that guide nanoscale motion. We report here observation of electromagnetic forces in groups of nanoscale metal particles, derived from the plasmonic response to the passage of a swift electron beam. At moderate impact parameters, the forces are attractive, toward the electron beam, in agreement with simple image charge arguments. For smaller impact parameters, however, the forces are repulsive, driving the nanoparticle away from the passing electron. Particle pairs are most often pulled together by coupled plasmon modes having bonding symmetry. However, placement of the electron beam between a particle pair pushes the two particles apart by exciting antibonding plasmonic modes. We suggest how the repulsive force could be used to create a nanometer-sized trap for moving and orienting molecular-sized objects.

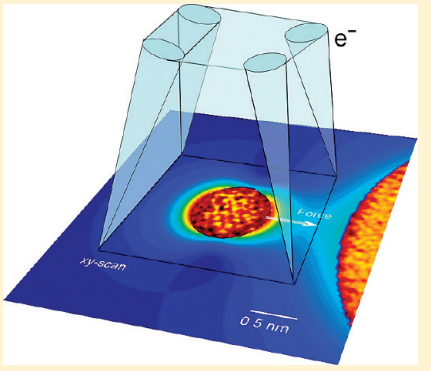

KEYWORDS: Plasmonics, plasmonic forces, optical forces, plasmon hybridization, aloof electron scattering, nanoparticle coalescence

During the past few years, increasing interest has been directed toward the plasmonic and photonic behavior of nanometer-sized metal and dielectric structures, to understand the coupling of light into subwavelength objects.[1] This coupling of optical energy into a confining structure results in enhanced local electric fields and can produce *forces* of tens of piconewtons, which have been widely used as "optical tweezers" to trap submicrometer sized particles.[2] If large enough, these forces also have the potential to alter local structure[3] or to encourage nanoscale self-assembly.[4] Scanning tunneling microscopy has also used subnanoscale electrostatic fields to trap and move atoms on low temperature surfaces.[5] These techniques use electromagnetic interactions to move or confine nanoscale objects—atoms, molecules, and particles—on nanometer distances. In the absence of external fields, the collective behavior of valence and atomic core electrons also produce similar behavior—London dispersion, Debye, and Keesom forces—which have been investigated for many years.[6] Thus, the controlled manipulation of external electromagnetic forces at nanometer and subnanometer length scales might lead to better understanding of the fundamental forces that hold all materials together.

Nonintersecting, or *aloof*, electron beam excitation of surface plasmons on surfaces and in nanoscale objects was first explored in the context of grazing incidence electron energy loss spectroscopy (EELS),[7] and soon after during the development of spatially resolved electron energy loss spectroscopy (srEELS) in the scanning transmission electron microscope (STEM).[8,9] Excellent reviews of the rich set of phenomena accessible to these spatially resolved experiments have been given.[10,11] Recently, exciting new experimental and theoretical work has continued these studies for photonic, plasmonic, and novel surface excitations.[12−18] With our increasing ability to produce angstrom-sized electron beams in the STEM,[19,20] it is now possible to investigate smaller particles, ranging in size down to single atoms. During this process, the particle is often modified: structurally altered, moved, or rotated under the electron beam.[21−23] Further, during the first use of subangstrom imaging, pairs of nanometer-sized Au particles were also observed to coalesce frequently.[23]

Received: May 26, 2011
Revised: July 17, 2011
Published: July 19, 2011

We have modeled this coalescent behavior theoretically, concluding that it is caused by attractive interparticle forces resulting from the coupling of surface plasmons on each particle, forming a lower energy plasmon mode having *bonding* symmetry.[8,24,25] This coupled behavior is also responsible for the large field enhancement that enables surface enhanced raman scattering in particle dimers.[26−28]

In this report, we discuss the controlled manipulation of 1−2 nm Au particles singly, in pairs, and as part of nanoparticle groups, allowing a surprising range of possibilities to control nanoscale motion. For single nanoparticles, we demonstrate long-ranged *attractive* and short-ranged *repulsive* forces between the electron beam and the Au particles. To understand this behavior, we have calculated forces which arise from dipole and multipole dielectric polarization of particles in response to a swift electron passing at a small impact parameter. In dimer nanoparticle systems, we show that coalescence can be induced or prevented by appropriate beam placement and explain this behavior in terms of bonding and antibonding plasmonic interparticle coupling, respectively.[24] Finally we suggest how the new repulsive behavior might be used to trap molecular-sized objects to move and rotate them on length scales of a few angstroms.

Experimental Method. In general, electron microscopy endeavors to minimize electron beam induced sample modification to obtain structure which is characteristic of the pristene material. In this experiment we have deliberately maximized conditions needed for modification to reveal mechanisms that promote movement. The nanoparticles are about 4× smaller than those commonly observed in the past. At 0.5−1.0 nm, in the presence of the carbon substrate, the smallest Au particles do not have compact perimeters, and their crystal structure is fluctuating among several possibilities, some of which are not stable in the bulk. The beam current density is also about 2× larger, and with the aberration corrected optics, the beam can be positioned closer to the nanoparticle than has been practical in the past. Even so, the detected movement of a single 1.5 nm nanoparticle at a distance of 4.5 nm from the electron beam is very small, about −0.03 nm/s as described in the Supporting Information, so these experiments require several tens of seconds for completion.

The experimental geometry is described in Figure 1A which shows an oblique view of image data for two Au nanoparticles on amorphous carbon. The data were recorded in a VG Microscopes, HB501 scanning transmission electron microscope, (STEM) fitted with a third-order aberration corrector to allow formation of a 0.8 Å electron beam at 120 keV acceleration energy.[20] The STEM forms images by scanning the small beam in an $x-y$ raster, using scattered electrons or other signals, to map materials structure. This *Scanned Area*, shown in Figure 1A (white lines), encloses small (<2 nm) target particles located within a larger *Neighborhood* which may include other, nonmoving large (>4 nm) particles. At the beginning of each line in the Scanned Area, the electron beam is stopped for about 20% of the line time, producing an *aloof* beam current density with respect to the Au particle, schematically illustrated by the pencil-shaped probe in the figure. Thus, the particles are influenced by the electron beam during $x-y$ scanning, but they also experience electric fields from a *Stopped Beam*, positioned at the beginning of each line, to the left of the Scanned Area. During this time, the particle experiences polarization fields imposed by the passing electron beam, averaged over a range of impact parameters measured from the particle to the left edge of the scanned area, denoted by the doubled line in Figure 1A. During $x-y$ scanning within the scanned

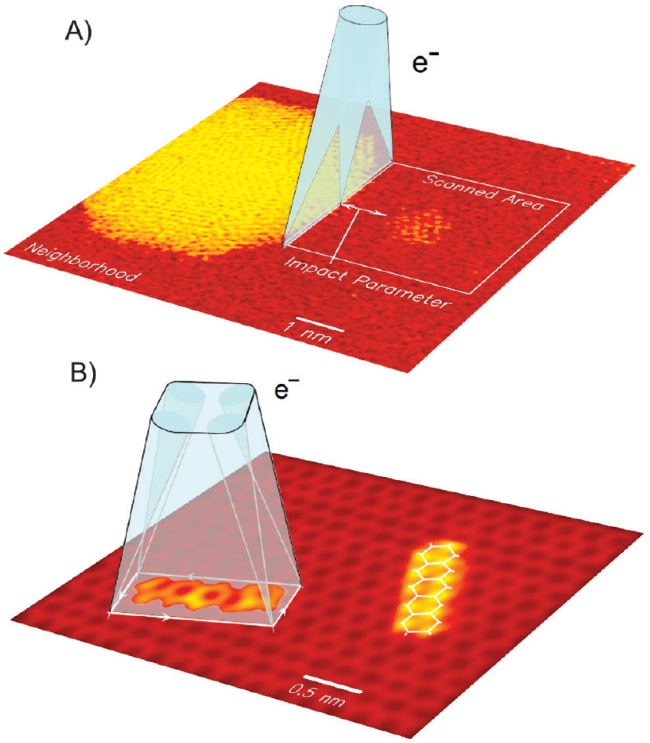

Figure 1. (A) Relationship of the passing electron beam with a Au particle pair. The *Neighborhood* may contain other particles of varying sizes. During the experimental observation, the electron beam is periodically motionless at the left edge of a *Scanned Area*, influencing the small particle with an impact parameter. This figure corresponds to the experiment described in Figure 5A below. (B) Suggested use of the discovered repulsive force to orient and move pentacene on a graphene sheet. One pentacene molecule is bonded to a low energy position on the graphene,[39] while the other is constrained by an electron beam designed for trapping. Image intensities are predicted using a frozen phonon multislice STEM simulation technique.[38].

area, the particle is directly sampled by the probe and experiences applied fields from many directions.[23] In Figure 1B, we show a similar view for a suggested trapping experiment, where the probe is scanned around the perimeter of a pentacene molecule on a graphene substrate, producing an *aloof* probe having a rectangular shape.

Theoretical Framework. In Figure 2B, we compare forces for single spheres with pairs of spheres[25] by evaluating the Maxwell stress tensor at the surface of a 1 nm radius sphere imposed by the total fields in the presence of a passing swift electron.[29] In Figure 2A, we show four candidate beam-particle geometries for single spheres and pairs of spheres. The instantaneous transverse force that results from electron passage can be significant, of order 2−20 pN, compared with the ∼70 pN continuous force obtained with optical tweezers.[2,3] Nanoparticles respond to a large number of these sharp impulse forces by occasionally moving from one stable place on the substrate to a new, nearby location. An unexpected result of the calculation is that while the force on a single sphere at moderate impact parameter is weakly attractive toward the electron beam (red curve), at small impact parameters it reverses sign, becoming strongly repulsive. This is surprising because a simple image charge model for an electron passing the surface of a metal predicts that the force should always be attractive. For small impact parameter, however, the

dx.doi.org/10.1021/nl201795u |*Nano Lett.* 2011, 11, 3388–3393

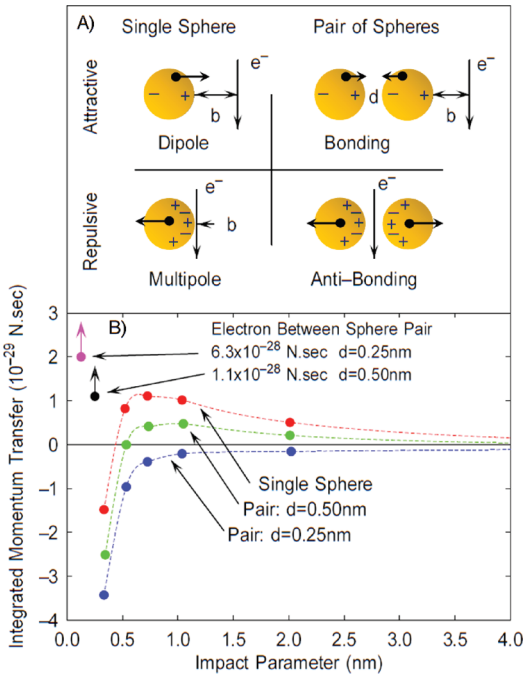

Figure 2. (A) Summary of four physical geometries tested in this work. These include repulsive and attractive forces, distinguishing between dipole and multipole modes in single spheres, and bonding and antibonding modes in pairs of spheres. (B) Transferred momentum for various nanoparticle situations, including an isolated 1 nm radius Au sphere (red), pairs of 1 nm radius spheres separated by d = 0.25 nm (blue) and 0.5 nm (green), for electron impact parameter, b. For the isolated sphere the momentum transfer is positive (toward the electron) for moderate impact parameter and negative (away from the electron) for small impact parameter. For a pair of spheres sufficiently close together, the momentum transfer is always negative, forcing the two spheres together. Positioning the electron beam between a pair (black and pink points) forces them apart.

electric field imposed by the electron has significant inhomogeneity, exciting shorter wavelength, multipole, modes which accompany the appearance of repulsive forces. In pairs of spheres close together, polarization having bonding character pulls the spheres together for electrons passing outside (blue curve), while antibonding polarization for paths between the spheres forces them apart (black and pink points). The green curve, for a pair separated by a larger distance, exhibits a behavior which is intermediate between a single sphere and a close pair of spheres. If the electron path is neither at the end of the particle pair nor precisely between them, a null result can occur. For instance, in the electrophoretic motion of spheres, application of electric fields at an angle of about 30° to the line joining a sphere pair produces a mix of bonding and antibonding electrostatic coupling, with no net force.[30] This correspondence of the electrophoretic behavior with the electron scattering results is a consequence of the largely electrostatic nature of induced plasmonic polarization forces. Thus, there is a very broad continuum of behavior supported by this plasmonic polarization mechanism.

Alternative mechanisms for nanoparticle movement under the electron beam include dielectric forces due to specimen charging via secondary electron generation, either directly or through surface or bulk plasmon decay,[31,32] direct momentum transfer due to electron diffraction,[33] or thermal diffusion caused by local heating.[22] None of these phenomena would produce the observed range of behavior.

Movement of a Single Nanoparticle. We begin discussing experimental results with Figure 3 where we show the movement of a 1.5 nm diameter nanoparticle in a geometry designed to minimize bonding attraction of the small particle with a larger neighbor, inspired by the electrophoretic example.[30] This allows the larger nanoparticle position to be used as a reference for the movement of the small particle under the influence of the electron beam alone. In Figure 3A, we use a 4.5 nm impact parameter, as defined in Figure 1A. In this case, the stopped probe position is out of the field of view on the left of the displayed image. In Figure 3B, the scanned area is denoted by the dashed box, reducing the impact parameter to ≈1 nm. Image data were obtained using 0.2 s frame times, with image frames identified by number and time stamp. As the particle moved, the scanned area was moved with the particle by hand. Occasionally, the scanned area was increased in size to obtain an image including the larger particle, allowing precise measurement of the small particle position relative to the center of the larger particle. The original position of the small particle is indicated by the vertical dotted line. Movie clips for these and subsequent experiments are available in the Supporting Information.

At 4.5 nm impact parameter, in Figure 3A, the smaller Au particle is pulled toward the left. On average, the motion is linear with time, about 0.03 nm/s, with pronounced scatter, of the order 0.1 nm rms. We believe that this motion is dominated by an excitation rate, proportional to beam current, resulting in movement to new bonding positions, directionally biased by the imposed force impulses. The very low excitation rate suggests that scattering events that transfer enough energy to overcome local bonding are relatively rare. In Figure 3B, at 1.0 nm impact parameter, we push the particle to the right, away from the stopped beam more rapidly—about 0.14 nm/s. Using the smaller scanned area to control the impact parameter, we also increase the average current density—about 4× in this case—thereby increasing the excitation rate, explaining the change in drift velocity. We have also increased the beam influence on the larger particle, causing a small rotation, shown in Figure 3B.

Movement of Pairs of Nanoparticles. As discussed in earlier work, pairs of 1−10 nm Au clusters readily coalesce under the electron beam.[23] Figure 4 shows two examples of this behavior, chosen to show that it is not very sensitive to the precise stopped beam location. In particular, it does not depend on which particle is oriented toward the stopped beam. In either case, the smaller particle is driven toward its larger neighbor. This is direct evidence that this behavior is not due to intrinsic charges located on the spheres or to charges caused by secondary electron emission but rather due to polarization charges induced by the passing beam.

If the stopped beam area is positioned between the two particles, as shown in Figure 5A, and summarized schematically in Figure 1A, the result is a plasmonic mode having antibonding character, driving the particles apart. In this illustration, the center image shows an overlay of data from the scanned area during the directed force experiment. Interestingly, another larger particle in the upper right participates in the polarization process, biasing the small particle movement toward that particle. On the basis of other observations, the eventual outcome of this movement would be coalescence of the small particle with the particle in the upper right.

Movement in Groups of Nanoparticles. In Figure 5B, we consider a more complex situation, with several particles. As

dx.doi.org/10.1021/nl201795u |*Nano Lett.* 2011, 11, 3388–3393

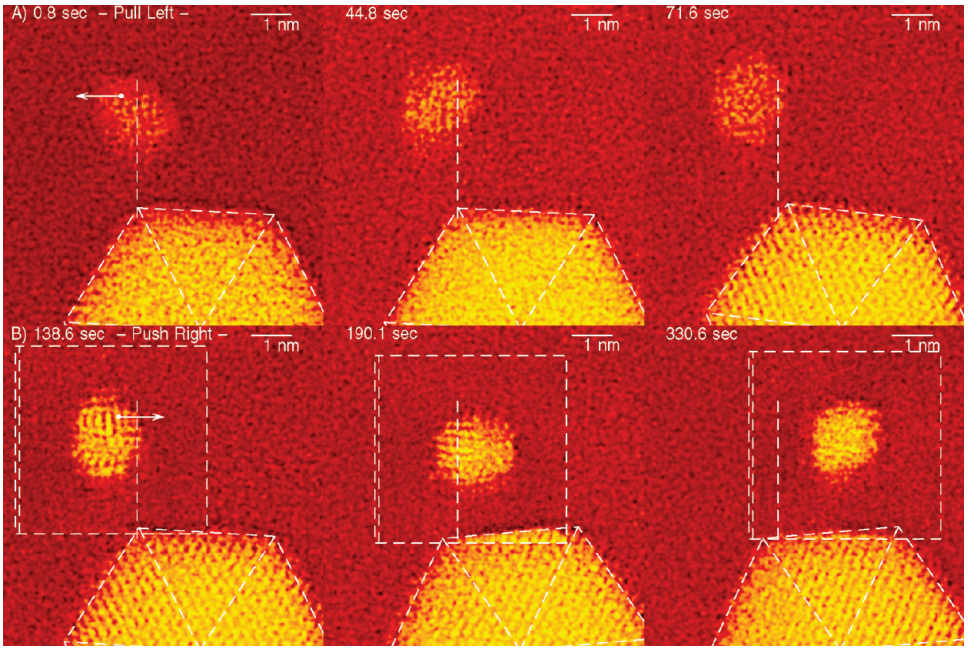

Figure 3. Directed motion of a 1.5 nm Au particle on amorphous carbon. (A) Pulling using a dipolar polarization of a single sphere induced by a moderate, 4.5 nm, impact parameter. (B) Pushing the same sphere using multipolar polarization induced by a 1 nm impact parameter. The scanning probe-pair geometry was chosen to minimize forces between the 1.5 nm particle and the lager 4.5 nm particle. Motion was measured relative to the center of the 4.5 nm particle. Time stamps identify image frames.

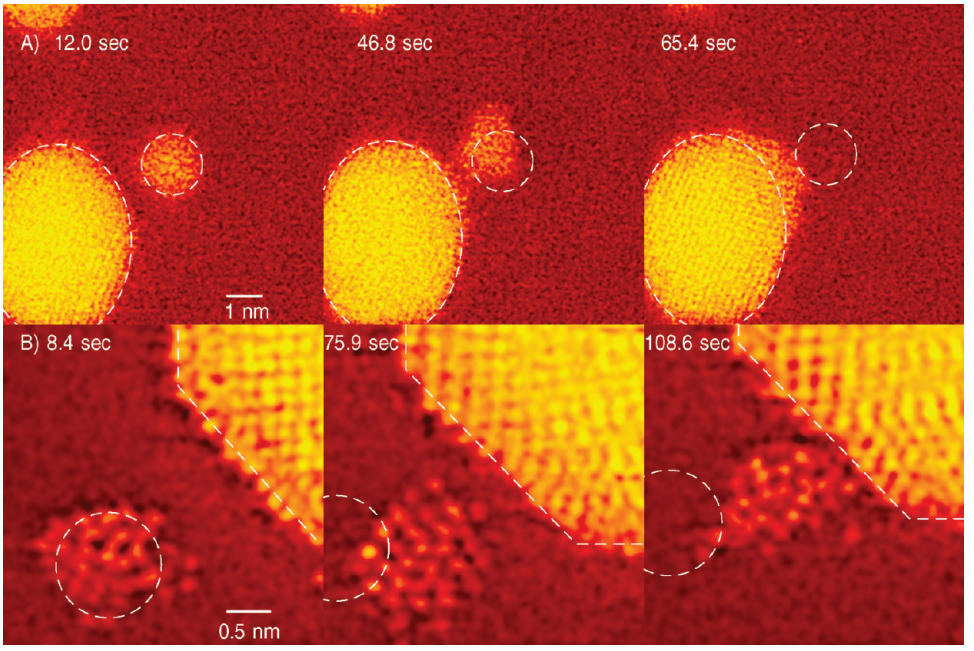

Figure 4. Coalescence of two nanometer-sized particles using bonding forces. When the stopped electron beam is largely to the left of (A) the larger particle or (B) the smaller particle. In each case, the motion favors coalescence by forcing the smaller particle into the larger. Time stamps identify image frames.

summarized in the middle panel, we position the scanned area so that the stopped beam drives a coalescent force for a particle pair in the lower left, (indicated by the arrows) but a separating force for the smaller particle. The right panel shows that the desired behavior, toward coalescence for one pair and separation for the other, was readily obtained with the understanding gained by observation of the simpler geometries in the previous examples. It is important to realize that, while the short ranged, repulsive forces are dominant in this example, the longer ranged dipolar field significantly influences the polarization behavior of the particle neighborhood.

Conclusions. In conclusion, this work identifies plasmonic forces as a source of movement in collections of nanoscale objects undergoing examination by electron microscopy. We have shown

dx.doi.org/10.1021/nl201795u |*Nano Lett.* 2011, 11, 3388–3393

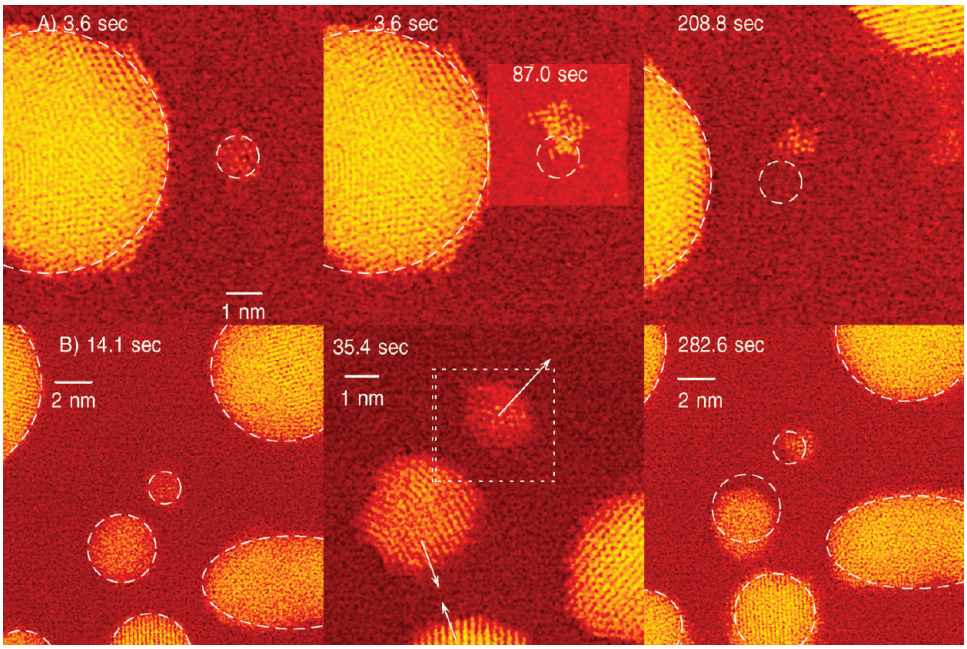

Figure 5. Movement of nanoparticles in more complicated situations. (A) When the stopped beam area is placed between two particles, antibonding polarization is induced and the smaller particle is forced away and, in this case, with a bias toward a neighboring particle. (B) When several particles lie within the neighborhood, multiple geometries occur, in this case, two moderately sized particles are pulled toward each other, while a third, smaller particle is pushed away. Time stamps identify image frames.

for the first time that both attractive and repulsive forces result from this, demonstrating deliberate manipulation of a single 1.5 nm Au nanoparticle, pairs of nanoparticles, and assemblies of several particles. These results are in agreement with calculations which predict a reversal of sign of the force at impact parameters comparable to the particle diameter. We see also variations with the impact parameter orientation in particle pairs (summarized in the Supporting Information), with the caution that many parameters in this experiment are challenging to control, including precision of the impact parameter, the beam current density, and the stopped beam position.

The reversal of the force in pairs, caused by the antibonding polarization for a beam position between the two spheres, is relatively strong, of order 10× the coalescent forces, as summarized in Figure 2B above. It also corresponds to the so-called dark-mode surface plasmon, excited when the beam is located between the two particles.[34] In the single particle case, the small impact parameter force reversal is accompanied by excitation of higher energy, short wavelength plasmonic modes, but at the present time, the detailed, microscopic explanation of the force reversal is the subject of ongoing effort to be reported later.

Aloof electron interaction at the nanoscale is a little like playing "billiards" with the nanoparticles, using many short pushes or pulls of billiard balls. Unlike billiards, however, the nanoparticle motion is limited by a large Stokes viscous drag caused by making and breaking bonds with the substrate, resulting in diffusive movement similar to Brownian motion, with the nonstochastic, directed electron impacts taking the role of random thermally driven atomic impacts for the Brownian case.[35] There are several ways that this behavior might be used to constrain and guide a nanoscale particle. It may be possible to shape the electron beam density, making a hollow cone that fits over a nanoscale object, trapping it using the small impact parameter push, in effect creating nanoscale "tweezers". Another possibility would be to trap the object by scanning the subangstrom probe along its perimeter. In this way, high aspect ratio objects could be oriented by rotating the perimeter scan, or they could be moved, with minimal direct impact by the electron beam. Pentacene, recently imaged using atomic force microscopy,[36] is a good example of a nanoscale object that might be manipulated in this way. In Figure 1B, we show a simulation of this possibility, using a calculated STEM image of two pentacene molecules on a graphene substrate using a frozen phonon multislice STEM technique.[37,38] One molecule is bonded to the graphene with half of its carbon atoms in registry with graphene atom positions.[39] The second is held by the beam at a nonequilibrium angle with respect to the substrate. A third method would be to use a low beam current in a raster scan to image a nanoscale object under low dose conditions, while periodically pulsing the beam current to a higher value in a pattern that will trap, guide, or orient a molecule or particle. The experiments reported here, where the beam is periodically held motionless at the edge of the raster scan, in a well-defined line, are examples of this kind of operation.

In general, *aloof* swift electron interaction allows us to identify common behavior of nanoscale systems under electric fields. These may be external applied fields or fields originating in nearby structures—for instance, the highly local fields that can result from valence changes at an interface.[40] We believe that the principles uncovered here are relevant to many other atomic and molecular phenomena. The appearance of a negative force between the electron beam and a nanoscale metal object at very small impact parameters is surprising and intriguing and illustrates that subangstrom electron beams present an extremely valuable tool for detailed investigation of the interaction of electric fields with molecular-sized objects. Finally, we think that this negative force will be useful in devising an electron-based trapping technique to manipulate atoms, molecules, and other nanoscale objects over angstrom-level distances.

dx.doi.org/10.1021/nl201795u |*Nano Lett.* 2011, 11, 3388–3393

■ ASSOCIATED CONTENT

Supporting Information. Additional information about the instrumentation used and procedures and videos showing variations with the impact parameter orientation in particle pairs. This material is available free of charge via the Internet at http://pubs.acs.org.

■ AUTHOR INFORMATION

Corresponding Author
*E-mail: batson@physics.rutgers.edu.

■ ACKNOWLEDGMENT

We acknowledge financial support from the Basic Energy Sciences Division of the Department of Energy, Award #DE-SC0005132, the Department of Industry of the Basque Government through the ETORTEK project inano, the Spanish Ministerio de Ciencia e Innovación through Project No. FIS2010-19609-C02-01, and the Consejo Nacional de Ciencia y tecnología (Mexico) through Project No. 82073. We also gratefully acknowledge support of the IBM Thomas J. Watson Research Center, Yorktown Heights, New York 10598, where the data reported here were obtained.

■ REFERENCES

(1) Barnes, W. L.; Dereux, A.; Ebbesen, T. W. *Nature* **2003**, *424*, 824–830.
(2) Ashkin, A.; Dziedzic, J. M.; Bjorkholm, J. E.; Chu, S. *Opt. Lett.* **1986**, *11*, 288–290.
(3) Hallock, A. J.; Redmond, P. L.; Brus, L. E. *Proc. Nat. Acad. Sci.* **2005**, *102*, 1280–1284.
(4) Smith, P. A.; Nordquist, C. D.; Jackson, T. N.; Mayer, T. S.; Martin, B. R.; Mbindyo, J.; Mallouk, T. E. *Appl. Phys. Lett.* **2000**, *77*, 1399–1401.
(5) Eigler, D. M.; Schweizer, E. K. *Nature* **1990**, *344*, 524–526.
(6) French, R. H. *J. Am. Ceram. Soc.* **2000**, *83*, 2117–2146.
(7) Warmack, R. J.; Becker, R. S.; Anderson, V. E.; Ritchie, R. H.; Chu, Y. T.; Little, J.; Ferrell, T. L. *Phys. Rev. B* **1984**, *29*, 4375–4381.
(8) Batson, P. E. *Phys. Rev. Lett.* **1982**, *49*, 936–940.
(9) Ferrell, T. L.; Echenique, P. M. *Phys. Rev. Lett.* **1985**, *55*, 1526–1529.
(10) Rivacoba, A.; Zabala, N.; Aizpurua, J. *Prog. Surf. Sci.* **2000**, *65*, 1–64.
(11) García de Abajo, F. J. *Rev. Mod. Phys.* **2010**, *82*, 209–275.
(12) Yurtsever, A.; Couillard, M.; Muller, D. A. *Phys. Rev. Lett.* **2008**, *100*, 217402.
(13) Nelayah, J.; Kociak, M.; Stephan, O.; García de Abajo, F. J.; Tence, M.; Henrard, L.; Taverna, D.; Pastoriza-Santos, I.; Liz-Marzan, L. M.; Colliex, C. *Nat. Phys.* **2007**, *3*, 348–353.
(14) García de Abajo, F. J.; Kociak, M. *Phys. Rev. Lett.* **2008**, *100*, 106804.
(15) Rossouw, D.; Couillard, M.; Vickery, J.; Kumacheva, E.; Botton, G. A. *Nano Lett.* **2011**, *11*, 1499–1504.
(16) Koh, A. L.; Fernández-Domínguez, A. I.; McComb, D. W.; Maier, S. A.; Yang, J. K. W. *Nano Lett.* **2011**, *11*, 1323–1330.
(17) Yamamoto, N.; Ohtani, S.; García de Abajo, F. J. *Nano Lett.* **2011**, *11*, 91–95.
(18) Diaconescu, B.; Pohl, K.; Vattuone, L.; Savio, L.; Hofmann, P.; Silkin, V. M.; Pitarke, J. M.; Chulkov, E. V.; Echenique, P. M.; Farias, D.; Rocca, M. *Nature* **2007**, *448*, 57–59.
(19) Haider, M.; Uhlemann, S.; Schwan, E.; Rose, H.; Kabius, B.; Urban, K. *Nature* **1998**, *392*, 768–769.
(20) Batson, P. E.; Dellby, N.; Krivanek, O. L. *Nature* **2002**, *418*, 617–620.
(21) Marks, L. D. *Rep. Prog. Phys.* **1994**, *57*, 603–649.
(22) Buffat, P. A. *Philosophical Transactions of the Royal Society of London. Series A: Mathematical, Physical and Engineering Sciences* **2003**, *361*, 291–295.
(23) Batson, P. E. *Micros. Microanal.* **2008**, *14*, 89–97.
(24) Prodan, E.; Radloff, C.; Halas, N. J.; Nordlander, P. *Science* **2003**, *302*, 419–422.
(25) Reyes-Coronado, A.; Barrera, R. G.; Batson, P. E.; Echenique, P. M.; Rivacoba, A.; Aizpurua, J. *Phys. Rev. B* **2010**, *82*, 235429.
(26) Batson, P. E. *Surf. Sci.* **1985**, *156*, 720–734.
(27) Xu, H.; Bjerneld, E. J.; Käll, M.; Börjesson, L. *Phys. Rev. Lett.* **1999**, *83*, 4357–4360.
(28) Klimov, V. V.; Guzatov, D. V. *Phys. Rev. B* **2007**, *75*, 024303.
(29) García de Abajo, F. J. *Phys. Rev. B* **2004**, *70*, 115422.
(30) Kang, K. H.; Li, D. *Langmuir* **2006**, *22*, 1602–1608PMID: 16460080.
(31) Mullejans, H.; Bleloch, A.; Howie, A.; Walsh, C. *Philosophical Magazine Letters* **1993**, *68*, 145–151.
(32) Pijper, F. J.; Kruit, P. *Phys. Rev. B* **1991**, *44*, 9192–9200.
(33) Marks, L.; Zhang, J. *Ultramicroscopy* **1992**, *41*, 419–422.
(34) Chu, M.-W.; Myroshnychenko, V.; Chen, C. H.; Deng, J.-P.; Mou, C.-Y.; García de Abajo, F. J. *Nano Lett.* **2009**, *9*, 399–404.
(35) Einstein, A. *Annalen der Physik* **1905**, *322*, 549–560.
(36) Gross, L.; Mohn, F.; Moll, N.; Liljeroth, P.; Meyer, G. *Science* **2009**, *325*, 1110–1114.
(37) Loane, R. F.; Xu, P.; Silcox, J. *Ultramicroscopy* **1992**, *40*, 121–138.
(38) Kirkland, E. J. *Advanced computing in electron microscopy*; Plenum Press: New York, 1998.
(39) Paramonov, P. B.; Coropceanu, V.; Brédas, J.-L. *Phys. Rev. B* **2008**, *78*, 041403.
(40) Muller, D. A. *Nat. Mater.* **2009**, *8*, 263–270.